Polyhedron 29 (2010) 296–302

Contents lists available at ScienceDirect

Polyhedron

journal homepage: www.elsevier.com/locate/poly

Luminescent zinc and cadmium metal-organic frameworks based on tetrazole ligands

Tuoping Hu [a,b], Longjie Liu [a], Xiaoli Lv [a], Xiaohui Chen [a], Haiyan He [a,*], Fangna Dai [a], Guoqing Zhang [a], Daofeng Sun [a,*]

[a] Key Lab of Colloid and Interface Chemistry, Ministry of Education, School of Chemistry and Chemical Engineering, Shandong University, Jinan 250100, PR China
[b] Department of Chemistry, North University of China, Taiyuan, Shanxi 030051, PR China

ARTICLE INFO

Article history:
Available online 13 May 2009

Keywords:
Tetrazole
Metal-organic framework
Fluorescence

ABSTRACT

Three metal-organic frameworks with 1D zigzag chain $[Zn(dte)(H_2O)_3]\cdot 2H_2O$ (**1**), 2D double layer $[Cd(dtb)(H_2O)(phen)]$ (**2**), 3D network $[Zn(dte)(phen)]$ (**3**) based on tetrazole-based ligands (H_2dtb = 1,3-dis(2H-tetrazol-5-yl)benzene, H_2dte = 1,4-ditetrazolylethylene, phen = 1,10-phenanthroline), have been synthesized and characterized. All the compounds exhibit unusual strong luminescence at room temperature in the solid state and can be potentially used as luminescent materials.

1. Introduction

The design and synthesis of molecular architecture with unusual structures and properties are now of great interest due to not only their intriguing molecular topologies, but also their potential applications as functional materials in many fields such as gas storage, catalysis, ion exchange, luminescence, nonlinear optics (NLO), magnetism [1–3]. The construction of supramolecular arrays relies on the combination of several factors [4–5]. Thus, it is a tremendous challenge to understand and control how these considerations influence the crystal packing and hence build the exactly predictable coordination supramolecular architectures. During past decades, great progress has been made in the rational design and controllable synthesis of such materials and a large number of compounds with interesting molecular structures and excellent properties according to some basic principles and feasible experiences have been successfully synthesized.

As an important kind of O-donor ligands, muticarboxylate ligands are widely used in the assembly of metal-organic frameworks due to their various coordination modes and bridging abilities [6–7]. Analogously, tetrazole-based ligands bearing alkyl spacers are a splendid option of N-donor ligands, and the four nitrogen atoms provide enough coordination sites when coordinating to metal centers with certain coordination geometries [8–13]. Previous studies show that these ligands exhibit special abilities to formulate the compounds and induce the final structures and topologies, and the results also indicate that tetrazole-based organic anions possess the similar coordination mode with poly-carboxylate ligand (Scheme 1) [14–16]. The common strategy for the construction of metal-organic frameworks with tetrazole ligands is based on *in situ* synthesis, that is, the synthesis of ligands and the coordination between the ligands and metal ions occur simultaneously. Although, it is convenient to get the complexes through one-pot hydrothermal reaction, it increases the difficulty to understand the factors that influence the formation of MOFs based on tetrazole-based ligands and survey the coordination mode of the metal-organic complexes. Consequently, inspired by Sharpless's pioneering work, we synthesized two tetrazole-based ligands, 1,3-dis(2H-tetrazol-5-yl)benzene (H_2dtb), 1,4-ditetrazolylethylene (H_2dte) [17–20], in which the H_2dte ligand was previously synthesized by Prof. Xiong through one-pot hydrothermal reaction [21]. By using above two organic ligands to assemble with metal ions, three new metal-organic supramolecules were obtained, in which the tetrazole groups possess similar coordination modes with carboxylates [21–24]. In this paper, we describe the detailed synthesis, structures and luminescence properties of three compounds, $[Zn(dte)(H_2O)_3]\cdot 2H_2O$ (**1**), $[Cd(dtb)(H_2O)(phen)]$ (**2**), $[Zn(dte)(phen)]$ (**3**), which possess 1D zigzag chain, 2D (4,4) net and 3D framework, respectively.

2. Experimental

All reagents and solvents for syntheses were purchased from commercial sources and used as received. The tetrazole ligands were synthesized in accordance with the procedure reported, shown in the Scheme 2 [18,25]. Elemental analyses (C, H, N) were obtained on a Perkin–Elmer 240 elemental analyzer. Photoluminescence spectra were performed on a Perkin Elmer LS 50B luminescence spectrometer.

* Corresponding authors.
E-mail addresses: hhy_83626@163.com (H. He), dfsun@sdu.edu.cn (D. Sun).

0277-5387/$ - see front matter Crown Copyright © 2009 Published by Elsevier Ltd. All rights reserved.
doi:10.1016/j.poly.2009.05.015

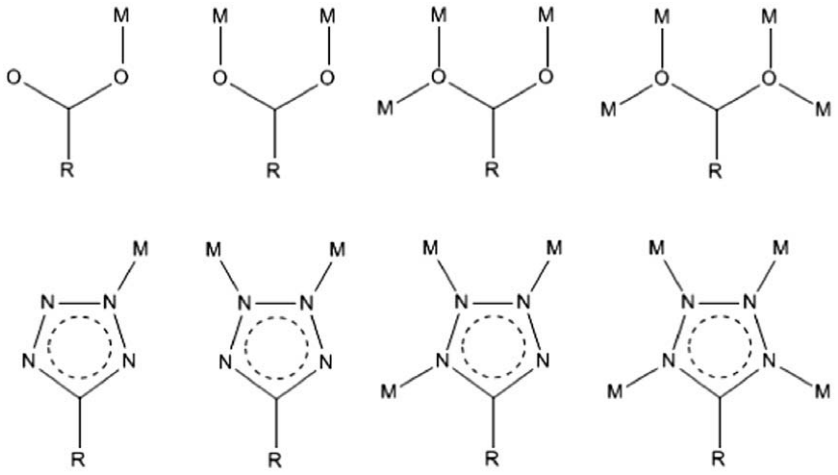

Scheme 1. Typical similar coordination modes for tetrazole ligand and carboxylate ligand.

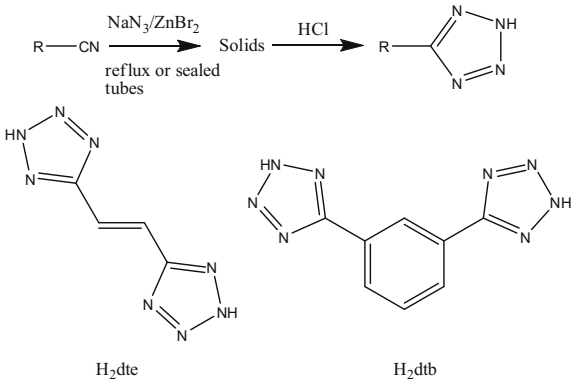

Scheme 2. The synthesis and the structures of two tetrazole ligand.

2.1. Syntheses of the metal complexes

2.1.1. Synthesis of $[Zn(dte)(H_2O)_3]\cdot 2H_2O$ (**1**)

A mixture of $Zn(NO_3)_2\cdot 6H_2O$ (20 mg, 0.07 mmol) and H_2dte (5 mg, 0.03 mmol) was suspended in the solution of H_2O (15 ml) and boiled for 10 minutes, and then the solution of phen (10 mg, 0.06 mmol) in 5 ml MeOH was added. The mixture was filtered and the filtrate was allowed to evaporate at room temperature for 3 days. The yellow block crystals (6 mg) were collected, washed with water and dried in the air. Yield: 64% (based on H_2dte). *Anal.* Calc. for $C_4H_{13}N_8O_5Zn$: C, 15.08; N, 35.17; H, 4.11. Found: C, 14.64; N, 35.89; H, 3.88%.

2.1.2. Synthesis of $[Cd(dtb)(H_2O)(phen)]$ (**2**)

A mixture of $Cd(NO_3)_2\cdot 4H_2O$ (20 mg, 0.06 mmol), H_2dtb (10 mg, 0.05 mmol) and phen (10 mg, 0.06 mmol) was suspended in the solution of H_2O (15 ml), and heated in a teflon-lined steel bomb at 150 °C for 3 days. The yellow needlelike crystals (13 mg) formed were collected, washed with water and dried in the air. Yield: 51% (based on H_2dtb). *Anal.* Calc. for $C_{20}N_{10}H_{14}OCd$: C, 45.94; N, 26.80; H, 2.68. Found: C, 45.93; N, 26.95; H, 2.705%.

2.1.3. Synthesis of $[Zn(dte)(phen)]$ (**3**)

A mixture of $Zn(NO_3)_2\cdot 6H_2O$ (20 mg, 0.07 mmol), phen (10 mg, 0.06 mmol) and H_2dte (5 mg, 0.03 mmol) was suspended in the solution of H_2O (15 ml), and heated in a teflon-lined steel bomb at 140 °C for 3 days. The yellow block crystals (7 mg) formed were collected, washed with water and dried in the air. Yield: 54% (based on H_2dte). *Anal.* Calc. for $C_{20}N_{10}H_{12}Zn$: C, 47.09; N, 34.34; H, 2.45. Found: C, 44.59; N, 33.89; H, 2.46%.

2.2. X-ray crystallography

Single-crystal X-ray diffraction data for compounds **1–3** were recorded on a Bruker APEXII CCD diffractometer with graphite-monochromated Mo Kα radiation (λ = 0.71073 Å) at room temperature. All the structures were solved by Direct Method of SHELXS-97 [26] and refined by full-matrix least squares techniques using the SHELXL-97 program [27] within WINGX [28]. The metal atoms in each complex were located from the E-maps, and other non-hydrogen atoms were located in successive difference Fourier syntheses and refined with anisotropic thermal parameters on F^2. The positions of H atoms were generated geometrically, assigned isotropic thermal parameters, and allowed to ride on their parent carbon atoms before the final cycle of refinement.

Table 1
Crystal data and the structure refinement for complexes **1–3**.

	1	2	3
Empirical formula	$C_4H_{11}N_8O_5Zn$	$C_{20}H_{14}CdON_{10}$	$C_{16}H_{10}N_{10}Zn$
Formula weight	316.58	522.81	407.71
Crystal system	monoclinic	monoclinic	monoclinic
Space group	*C*2/*c*	*P*2(1)/c	*C*2/*c*
a (Å)	11.496(2)	8.447(1)	18.729(2)
b (Å)	7.271(1)	12.221(2)	10.954(1)
c (Å)	15.050(3)	19.952(2)	7.678(1)
α (°)	90.00	90.00	90.00
β (°)	108.331(1)	94.058(1)	101.002(1)
γ (°)	90.00	90.00	90.00
V (Å^3)	1194.26(4)	2054.63(5)	1546.39(3)
Z	4	4	4
ρ_{calc}/g cm^{-3}	1.761	1.690	1.751
μ (mm^{-1})	2.087	1.099	1.616
F(0 0 0)	644	1040	824
θ Range/deg	2.85/32.25	1.96/27.44	2.16/27.47
Number of reflections collected	7664	4672	10 365
Number of independent reflections	1770	3420	1768
Number of restraints/parameters	0/103	0/289	0/123
Goodness-of-fit (GOF) on F^2	1.262	0.691	1.026
T (K)	273(2)	273(2)	293(2)
R_{int}	0.0232	0.0584	0.0248
R_1	0.0224	0.0362	0.0222
wR_2	0.0704	0.1580	0.0628

Table 2
Selected bond distances (Å) and angles (deg) for complexes **1–3**.

1		
Zn O1 1.9833(17)	Zn N1 2.0628(12)	Zn O3 2.0833(14)
Zn N1 2.0628(12)	Zn O3 2.0833(14)	
O1 Zn N1 106.01(3)	O1 Zn N1 106.01(3)	N1 Zn N1 147.98(6)
O1 Zn O3 95.53(5)	N1 Zn O3 87.19(6)	N1 Zn O3 89.76(5)
O1 Zn O3 95.53(5)	N1 Zn O3 89.76(5)	N1 Zn O3 87.19(6)
O3 Zn O3 168.94(10)		
2		
O Cd 2.446(4)	Cd N6 2.289(4)	Cd N2 2.288(4)
Cd N9 2.337(4)	Cd N10 2.346(4)	Cd N7 2.381(4)
N6 Cd N2 97.30(14)	N6 Cd N9 96.25(16)	N2 Cd N9 166.14(15)
N6 Cd N10 161.52(15)	N2 Cd N10 96.08(14)	N9 Cd N10 71.42(14)
N6 Cd N7 93.95(13)	N2 Cd N7 85.64(14)	N9 Cd N7 90.51(14)
N10 Cd N7 99.73(14)	N6 Cd O 87.79(13)	N2 Cd O 89.00(14)
N9 Cd O 94.46(13)	N10 Cd O 79.76(13)	N7 Cd O 174.53(12)
3		
Zn N3 2.1301(13)	Zn N3 2.1301(13)	Zn N5 2.1815(13) 2
Zn N5 2.1815(13)	Zn N2 2.2559(13)	Zn N2 2.2559(13)
N3 Zn N3 96.73(7)	N3 Zn N5 169.77(5)	N3 Zn N5 93.47(5)
N3 Zn N5 93.47(5)	N3 Zn N5 169.77(5)	N5 Zn N2 89.89(5)
N3 Zn N2 90.43(5)	N3 Zn N2 92.41(5)	N5 Zn N2 86.75(5)
N3 Zn N2 92.41(5)	N3 Zn N2 90.43(5)	N5 Zn N2 86.75(5)
N5 Zn N2 89.89(5)	N2 Zn N2 175.73(6)	

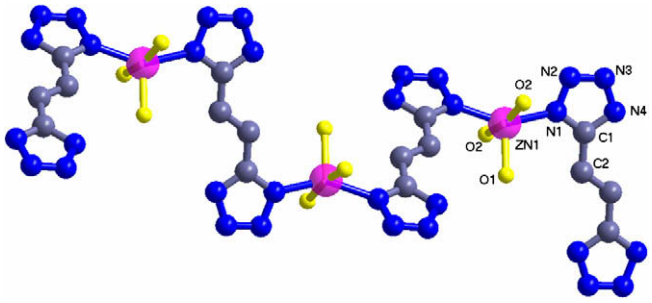

Fig. 1. Coordination environment of the zinc ion in and view of the chains.

3. Results and discussion

3.1. Descriptions of crystal structures

3.1.1. Structure of [Zn (dte) $(H_2O)_3$]·$2H_2O$ (**1**)

Single-crystal X-ray diffraction reveals that complex **1** is a one-dimensional zigzag chain with the asymmetric unit consisting of 1 zinc ion, 1 dte ligand, 1.5 coordinated water molecules and 1 uncoordinated water molecule (Tables 1 and 2). The central zinc ion is five coordinated by two nitrogen atoms from different dte ligands and three coordinated water molecules with the average Zn–N and Zn–O distances of 2.064 and 2.053 Å, respectively. The metal environment can be best described as a distorted tetragonal pyramidal, with two nitrogen atoms and two coordinated water molecules comprising the equatorial plane and one coordinated water molecule occupying the axial position. The two tetrazole groups are deprotonated during the reaction and the whole ligand acts as a bridging linker to connect two zinc ions to result in the formation of a one-dimensional zigzag chain structure, as shown in Fig. 1. The nearest Zn–Zn distance in the 1D zigzag chain is 8.566 Å. The dte ligand is almost planar with the dihedral angle between the two tetrazole groups of 54°.

The coordinated and uncoordinated water molecules as well as the uncoordinated nitrogen atoms of the dte ligand provide rich hydrogen donors and acceptors, respectively. Indeed, there are multiple supramolecular interactions existed in complex **1**. The $\pi\cdots\pi$ interactions (3.360 Å) between the tetrazole rings of dte in different zigzag chains connect the one-dimensional chains to form a two-dimensional layer with the nearest Zn–Zn distance in adjacent chains of 8.840 Å, as shown in Fig. 2a. The hydrogen bonding interactions (2.809 Å) between the coordinated water and the uncoordinated nitrogen atom of dte ligand, as well as the strong $\pi\cdots\pi$ interactions (3.383 Å) between tetrazole rings in different layers, further connect the two-dimensional layers to generate a three-dimensional supramolecular architecture, as shown in Fig. 2b.

3.1.2. Structure of [Cd(dtb)(H_2O)(phen)] (**2**)

Complex **2** is a two-dimensional layer framework based on binuclear cadmium unit. The asymmetric unit consists of one cadmium ion, one dtb ligand, one phen and one coordinated water molecule (Tables 1 and 2). The cadmium atom in **2** exhibits a distorted octahedral geometry (Fig. 3) with two nitrogen atoms from phen and two nitrogen atoms from different dtb ligand comprising the equatorial plane, while one coordinated water molecule and one nitrogen atom from dtb ligand occupying the axial position. The average Cd–N and Cd–O distances are 2.328 and 2.446 Å, in agreement with other cadmium complexes [29–31].

The dtb ligand in **2** is almost planar with the average dihedral angle between the central benzene ring and the side tetrazole rings of 15.6°. The two tetrazole groups of dtb ligand possess different

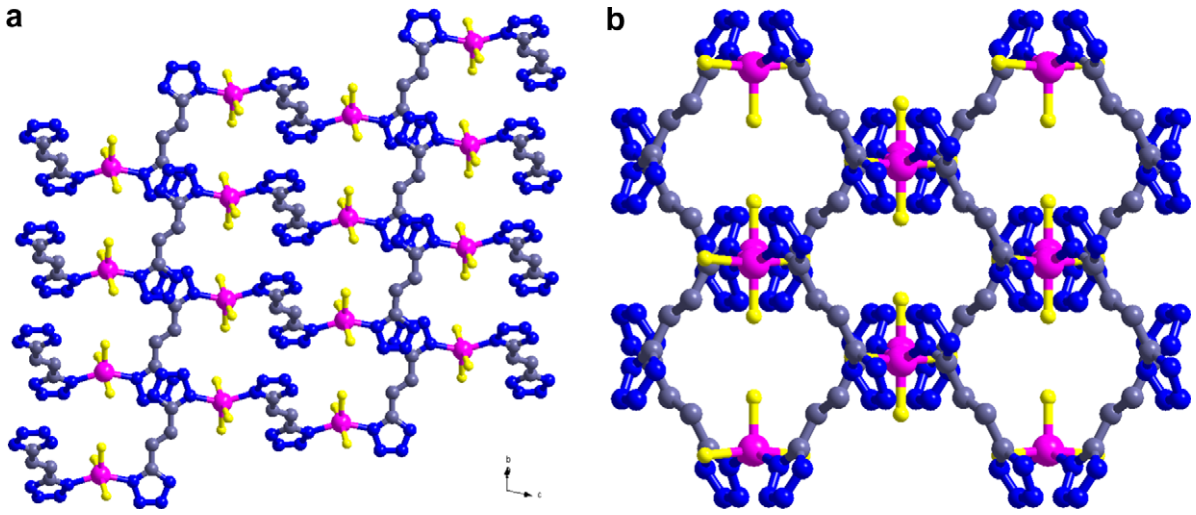

Fig. 2. (a) The whole view of the zigzag chain along [1 1 0] direction, (b) view of the supramolecular architecture along [0 0 1] direction.

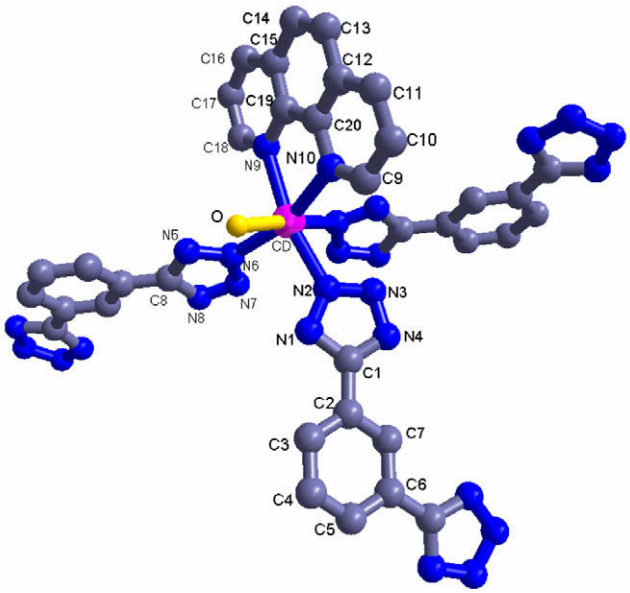

Fig. 3. Coordination environment of the cadmium cation in complex **2**.

coordination modes: one tetrazole group adopts didentate bridging mode to link two cadmium ions to form a binuclear unit, while the other tetrazole group adopts monodentate bridging mode to connect one binuclear cadmium unit. The binuclear cadmium unit can be considered as the basic building block of the whole framework. Thus, the binuclear building blocks are infinitely connected by the dtb ligands to generate a two-dimensional grid-like layer, as shown in the Fig. 4a. Two coordinated phen ligands locate in the quadrate grid by forming strong $\pi\cdots\pi$ interactions each other. While the coordinated water molecules point out of the layer, providing hydrogen bonding donors. It should be noted that, if the binuclear cadmium unit can be considered as a single node and the dtb as a linear linker, then complex **2** has a (4,4) net, similar to other reported complexes [32–34].

In the two-dimensional (4,4) layer, the dtb ligands connect the cadmium ions along *b*-axis to generate a one-dimensional 2_1 left- or right-handed helical chain with the nearest Cd–Cd distance of 11.328 Å (Fig. 4b). Thus, the two-dimensional layer can also be considered as formed by infinitely connection of the helical chains by sharing the binuclear cadmium unit. The left- and right-handed 2_1 helical chains are equal in the layer, thus, the whole structure is achiral.

As mentioned above, the coordinated water molecules provide the hydrogen bonding donors. The coordinated water molecules locate above or below the 2D layer and point out of the layer. Thus, the two-dimensional grid-like layers stacked one another through the hydrogen bonding interactions (2.871 Å) between the coordinated water molecules and the uncoordinated nitrogen atoms of dtb in different layers, giving rise to a three-dimensional supramolecular architecture (Fig. 4c). The coordinated phen ligands locate in the quadrate channels.

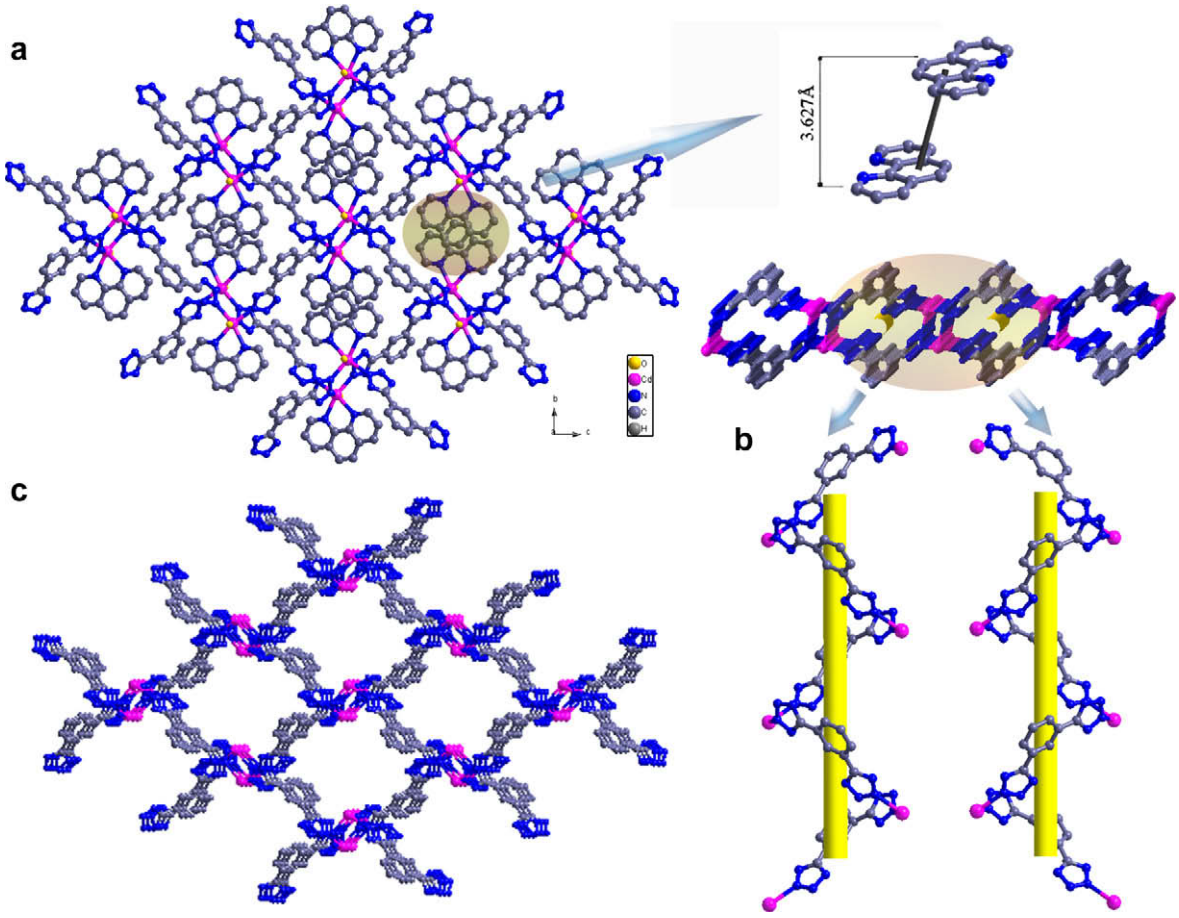

Fig. 4. (a) View of the double-layer from a axis and the highlight shows that the strong $\pi\cdots\pi$ interactions of phen ligands, (b) one-dimensional 2_1 left- or right-handed helical chain and (c) view of the quadrate channels in three-dimensional supramolecular architecture (coordinated phen ligands are omitted for clarity).

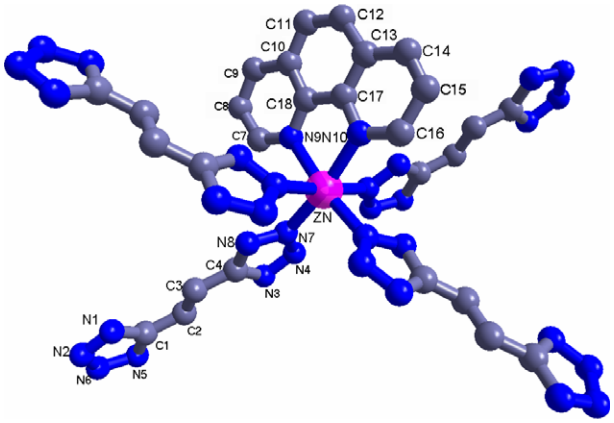

Fig. 5. Coordination environment of the zinc cation in complex **3**.

3.1.3. Structure of [Zn(dte)(phen)] (**3**)

Single-crystal X-ray diffraction studies show that complex **3** is a three-dimensional metal-organic framework. The asymmetric unit of **3** consists of one zinc ion, one dte ligand and one phen ligand, as shown in Fig. 5. The central zinc ion is six-coordinated by four nitrogen atoms from different dte ligands, two nitrogen atoms from the chelating phen ligand (Tables 1 and 2). The coordination geometry of the central zinc ion can be best described as a distorted octahedron, where two nitrogen atoms from phen ligand and two nitrogen atoms from different dte ligands comprise the equatorial plane, and the other two nitrogen atoms from another two different dte ligands occupying the axial positions with the angle of axial N–Zn–N of 173.99°.

Each phen acts as typical chelating ligand terminally coordinating to Zn ion with the average Zn–N distance and N–Zn–N angle being 2.178 Å and 76.26°, respectively. The average Zn–N distance (N from dte) is 2.194 Å, which is longer than that in **1**, probably due to the larger space hindrance from phen ligand in **3** as compared to coordinated water molecules in **1**. Both of tetrazole groups of dte ligand are deprotonated during the reaction, and each adopts didentate bridging mode to connect two zinc ions. Thus, every tetrazole group links two zinc ions and each zinc ion attaches to four tetrazole groups to form a one-dimensional chain, which is further connected by the backbone of dte to generate a three-dimensional metal-organic framework. The whole network structure can be viewed as consisting of regular rhombus in which apexes are occupied by zinc ions and the edges are formed by dte ligands (Fig. 6a). The phen ligands coordinating to the zinc ions penetrate in the cavity of the rhombus, thus the three-dimensional metal-organic framework of **3** can also be regarded as rhombus channels filled by phen ligands which are parallel to each other through $\pi\cdots\pi$ interactions (3.5 Å). The dimensions of the channels are about 18.38×8.90 Å based on the adjacent Zn–Zn distances [22] (Fig. 6b). The overall topology of **3** is similar with the coordination polymer of $[Mn(ta)(phen)]_n$ based on 1,4-benzenedicarboxylic acid ligand, which further indicates that tetrazole group possesses similar coordination modes with the carboxylates [22].

3.2. Luminescent properties

Coordination polymers are investigated for luminescence properties owing to their often higher thermal stability than the pure organic ligand and the ability of affecting the emission wavelength of the ligand by metal coordination. The combination of organic

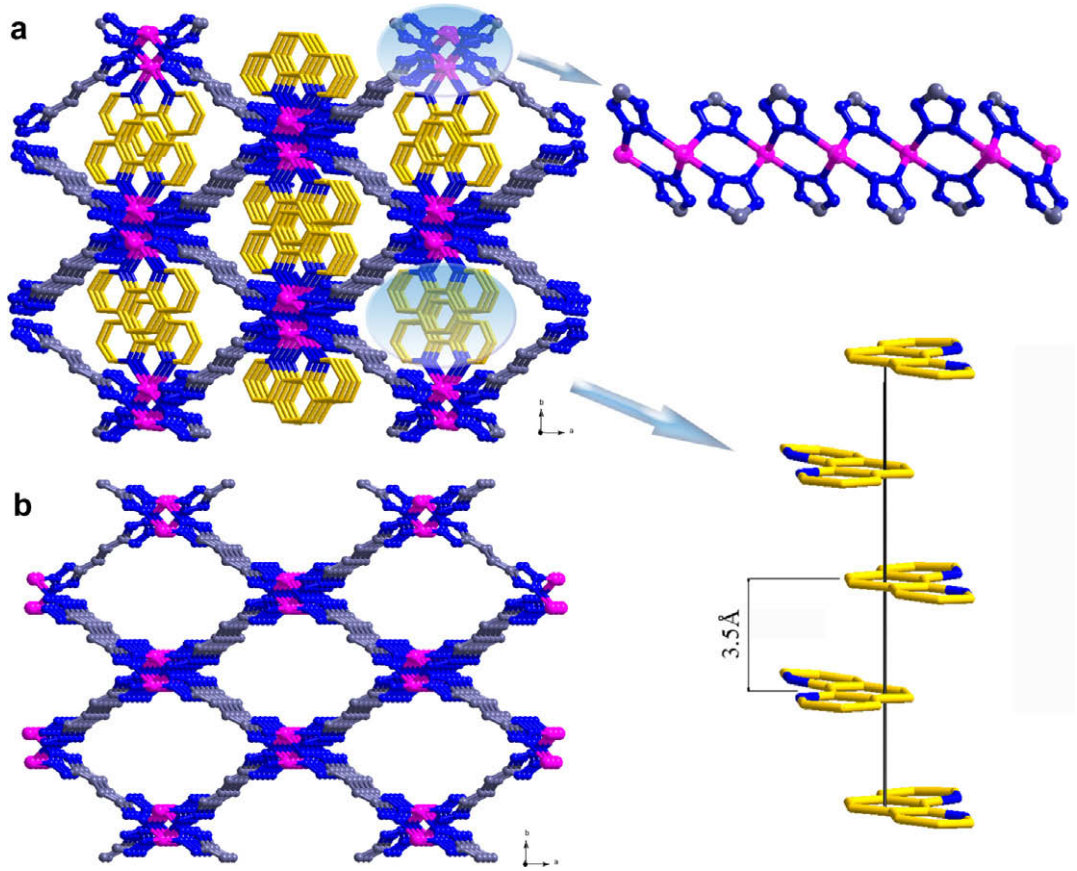

Fig. 6. (a) The 3D framework of **3** from *c* axis, the highlights show the coordination chain between metal and the ligands from *b*-axis, and the $\pi\cdots\pi$ interactions of phen ligands, respectively; (b) view of the channels of **3** along *c*-axis (coordinated phen ligands are omitted for clarity).

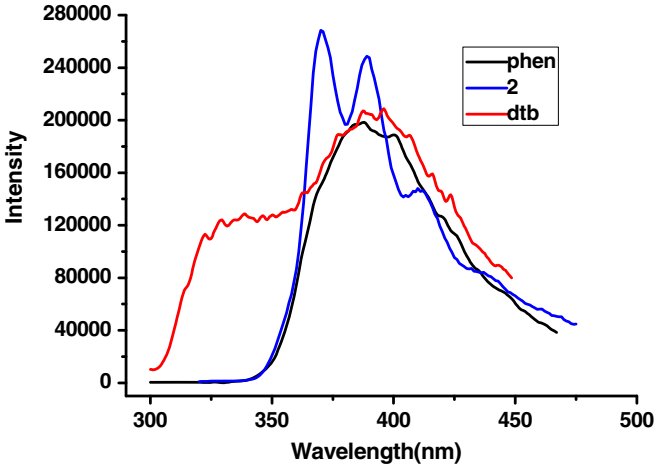

Fig. 7. Solid-state emission spectra of **2** at room temperature.

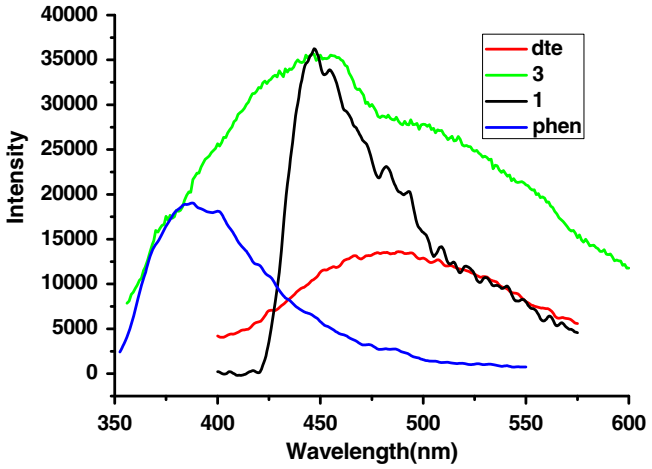

Fig. 8. Solid-state emission spectra of **1** and **3** at room temperature.

spacers and transition-metal centers in the coordination frameworks can be viewed as an efficient method for obtaining new types of luminescent materials for potential applications, e.g. chemical sensors, photochemistry, and electroluminescent display [35,36].

On the basis of current research of luminescent MOFs, the emission of metal-organic frameworks can be assigned to a ligand-to-metal charge-transfer (LMCT), metal-to-ligand charge transfer (MLCT) or an intraligand $\pi \rightarrow \pi^*$ transition [37]. The solid state photoluminescent spectra of free dtb, dte and phen measured at room temperature show the emission maxima at 396 nm for dtb, 488 nm for dte, and 388 nm for phen (Fig. 7 and 8). The emissions of the dtb, dte and phen ligands are assigned to intraligand $n \rightarrow \pi^*$ and $\pi \rightarrow \pi^*$ transitions.

Compared to the free ligands, the emission spectra of metal-organic frameworks of **1–3** changed. The emission band by coordination polymer **2** as compared to the emission band of the free ligands dtb and phen is quite unexpected. A broad and strong emission in the violet-blue region with maximum at 368 and a shoulder at 395 nm is observed as well as another weak emission at 420 nm (Fig. 7). These two emission bands, 368 and 420 nm, are red-shifted compared to free dtb or phen, and this may be ascribed to the ligand-to-metal charge-transfer (LMCT). Indeed, the emission band, 395 nm, is essentially unshifted from the maximum for free ligands, dtb and phen, which can still be assigned to intraligand transitions.

Complex **1** based on dte shows the emission maxima at 470 nm, while complex **3** based on dte and phen exhibits the emission maxima at 485 nm (Fig. 8). Both complexes **1** and **3** have a broad and strong emission band and complex **3** has a broader one, which may be due to the intraligands of mixed ligands in **3**. In addition, an obvious enhancement in the fluorescent intensity is observed. The emissions that occurred in **1** and **3** can be attributed to the ligand-to-metal charge-transfer (LMCT).

4. Conclusion

In this work, we have successfully synthesized three luminescent metal-organic frameworks with 1D zigzag chain of **1**, 2D layer

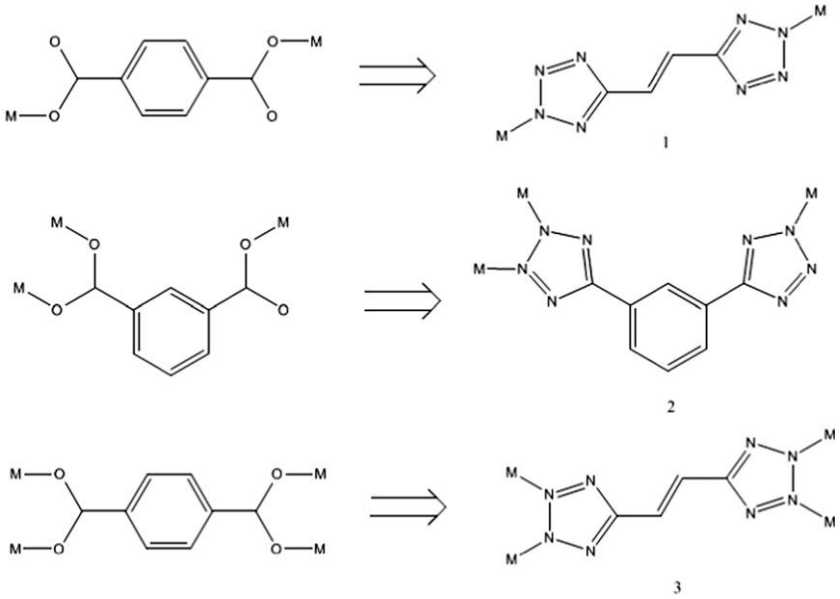

Scheme 3. The comparison of coordination modes between tetrazole ligands and carboxylate ligands.

of **2**, and 3D network of **3**, based on tetrazole ligands of 1,3-dis (2H-tetrazol-5-yl)benzene (H_2dtb) and 1,4-ditetrazolylethylene (H_2dte). In **1** and **2**, the supramolecular interactions such as hydrogen bond and $\pi\cdots\pi$ interactions play important roles in the formation of 3D supramolecular architectures. Complex **3** possesses the similar topology with the reported $[Mn(ta)(phen)]_n$ complex based on 1,4-benzenedicarboxylic acid, indicating the dte ligand plays the same role with ta ligand in the formation of these complexes. Our research shows that the tetrazole ligand possesses the similar coordination modes (Scheme 3), and properties with the corresponding carboxylate ligands in the construction of metal-organic frameworks. The photoluminescence investigation shows that all the coordination polymers **1–3** and corresponding free ligands are luminescent in the solid state and can be potentially applied as new luminescent materials.

Supplementary data

CCDC 723831–723833 contain the supplementary crystallographic data for **1–3**. These data can be obtained free of charge via http://www.ccdc.cam.ac.uk/conts/retrieving.html, or from the Cambridge Crystallographic Data Centre, 12 Union Road, Cambridge CB2 1EZ, UK; fax: (+44) 1223-336-033; or e-mail: deposit@ccdc.cam.ac.uk.

References

[1] O.M. Yaghi, C.E. Davis, H. Li, J. Am. Chem. Soc. 119 (1997) 2861.
[2] C. Janiak, J. Kim, N. Rosi, D. Vodak, J. Wachter, M. O'Keeffe, O.M. Yaghi, Dalton Trans. (2003) 2781.
[3] K. Barthelet, J. Marrot, D. Riou, G. Férey, Angew. Chem. Int. Ed. 41 (2002) 281.
[4] M. Munakata, L.P. Wu, T. Kuroda-Sowa, M. Maekawa, K. Moriwaki, S. Kitagawa, Inorg. Chem. 36 (1997) 5416.
[5] L. Carlucci, G. Ciani, P. Macchi, D.M. Proserpio, A. Sironi, Chem. Commun. (1997) 631.
[6] C.N.R. Rao, S. Natarajan, R. Vaidhyanathan, Angew. Chem. Int. Ed. 43 (2004) 1466.
[7] X.-L. Wang, C. Qin, E.-B. Wang, Z.-M. Su, Chem. Eur. J. 12 (2006) 2680.
[8] G.-H. Cui, J.-R. Li, J.-L. Tian, X.-H. Bu, S.R. Batten, Cryst. Growth Des. 5 (2005) 1775.
[9] R.-G. Xiong, Xiang. Xue, H. Zhao, X.-Z. You, B.F. Abrahams, Z.-L. Xue, Angew. Chem. Int. Ed. 41 (2002) 3800.
[10] L. Cheng, W.-X. Zhang, B.-H. Ye, J.-B. Lin, X.-M. Chen, Eur. J. Inorg. Chem. (2007) 2668.
[11] M. Dincă, A. Dailly, J.R. Long, Chem. Eur. J. 14 (2008) 10280.
[12] W.-L. Zhang, Y.-Y. Liu, J.-F. Ma, H. Jiang, J. Yang, Polyhedron 27 (2008) 3351.
[13] H. Park, G. Krigsfeld, S.J. Teat, J.B. Parise, Cryst. Growth Des. 7 (2007) 1343.
[14] M. Dincă, A.F. Yu, J.R. Long, J. Am. Chem. Soc. 128 (2006) 8904.
[15] M. Dincă, T.D. Harris, A.T. Iavarone, J.R. Long, J. Mol. Struct. 890 (2008) 139.
[16] C. Jiang, Z.-P. Yu, C. Jiao, S.-J. Wang, J.-M. Li, Z.-Y. Wang, Y. Cui, Eur. J. Inorg. Chem. (2004) 4669.
[17] S.J. Wittenberger, B.G. Donner, J. Org. Chem. 58 (1993) 4139.
[18] Z.P. Demko, K.B. Sharpless, J. Org. Chem. 66 (2001) 7945.
[19] M.L. Kantam, K.B.S. Kumar, Ch. Sridhar, Adv. Synth. Catal. 347 (2005) 1212.
[20] W. Ouellette, B.S. Hudson, J. Zubieta, Inorg. Chem. 46 (2007) 4887.
[21] X.-F. Huang, Y.-M. Song, Q. Wu, Q. Ye, X.-B. Chen, R.-G. Xiong, X.-Z. You, Inorg. Chem. Commun. 8 (2005) 58.
[22] D.-F. Sun, R. Cao, Y.-C. L, Q. Shi, W.-P. Su, M.-C. Hong, Dalton Trans. (2001) 2335.
[23] A.-L. Cheng, N. Liu, J.-Y. Zhang, E.-Q. Gao, Inorg. Chem. 46 (2007) 1034.
[24] R.-Q. Zou, L. Jiang, H. Senoh, N. Takeichi, Q. Xu, Chem. Commun. (2005) 3526.
[25] M. Dincă, A. Dailly, Y. Liu, C.M. Brown, D.A. Neumann, J.R. Long, J. Am. Chem. Soc. 128 (2006) 16876.
[26] G.M. Sheldrick, SHELXS-97 Programs for X-ray Crystal Structure Solution, University of Götingen, Götingen, Germany, 1997.
[27] G.M. Sheldrick, SHELXL-97, Programs for X-ray Crystal Structure Refinement, University of Götingen, Götingen, Germany, 1997.
[28] L.J. Farrugia, WINGX, A Windows Program For Crystal Structure Analysis, University of Glasgow, Glasgow, UK, 1988.
[29] B.-H. Ye, B.-B. Ding, Y.-Q. Weng, X.-M. Chen, Cryst. Growth Des. 5 (2005) 801.
[30] X. Shi, G.-S. Zhu, Q.-R. Fang, G. Wu, G. Tian, R.-W. Wang, D.-L. Zhang, M. Xue, S.-L. Qiu, Eur. J. Inorg. Chem. (2004) 185.
[31] Y.-Q. Lan, S.-L. Li, J.-S. Qin, D.-Y. Du, X.-L. Wang, Z.-M. Su, Q. Fu, Inorg. Chem. 47 (2008) 10600.
[32] Y.-M. Xie, J.-H. Liu, X.-Y. Wu, Z.-G. Zhao, Q.-S. Zhang, F. Wang, S.-C. Chen, C.-Z. Lu, Cryst. Growth Des. 8 (2008) 3914.
[33] E. Yang, J. Zhang, Z.-J. Li, S. Gao, Y. Kang, Y.-B. Chen, Y.-H. Wen, Y.-G. Yao, Inorg. Chem. 43 (2004) 6525.
[34] D. Krishna Kumar, D.A. Jose, A. Das, P. Dastidar, Inorg. Chem. 44 (2005) 6933.
[35] Q. Wu, M. Esteghamatian, N.-X. Hu, Z. Popovic, G. Enright, Y. Tao, M. D'Iorio, S. Wang, Chem. Mater. 12 (2000) 79.
[36] J.E. McGarrah, Y.-J. Kim, M. Hissler, R. Eisenberg, Inorg. Chem. 40 (2001) 4510.
[37] G.D. Santis, L. Fabbrizzi, M. Licchelli, A. Poggi, A. Taglietti, Angew. Chem., Int. Ed. Engl. 35 (1996) 202.